Type I interferon dependence of plasmacytoid dendritic cell activation and migration

Carine Asselin-Paturel,[1] Géraldine Brizard,[1] Karine Chemin,[1] Andre Boonstra,[2] Anne O'Garra,[2] Alain Vicari,[1] and Giorgio Trinchieri[1]

[1]Laboratory for Immunological Research, Schering-Plough Research Institute, Dardilly 69571, France
[2]Division of Immunoregulation, The National Institute for Medical Research, London NW7 1AA, England, UK

Differential expression of Toll-like receptor (TLR) by conventional dendritic cells (cDCs) and plasmacytoid DC (pDCs) has been suggested to influence the type of immune response induced by microbial pathogens. In this study we show that, in vivo, cDCs and pDCs are equally activated by TLR4, -7, and -9 ligands. Type I interferon (IFN) was important for pDC activation in vivo in response to all three TLR ligands, whereas cDCs required type I IFN signaling only for TLR9- and partially for TLR7-mediated activation. Although TLR ligands induced in situ migration of spleen cDC into the T cell area, spleen pDCs formed clusters in the marginal zone and in the outer T cell area 6 h after injection of TLR9 and TLR7 ligands, respectively. In vivo treatment with TLR9 ligands decreased pDC ability to migrate ex vivo in response to IFN-induced CXCR3 ligands and increased their response to CCR7 ligands. Unlike cDCs, the migration pattern of pDCs required type I IFN for induction of CXCR3 ligands and responsiveness to CCR7 ligands. These data demonstrate that mouse pDCs differ from cDCs in the in vivo response to TLR ligands, in terms of pattern and type I IFN requirement for activation and migration.

CORRESPONDENCE
Giorgio Trinchieri:
trinchig@niaid.nih.gov

Abbreviations used: cDC, conventional DC; CpG-ODN, oligonucleotides containing CpG motif; DC, dendritic cell; IFNAR$^{-/-}$, type I IFN receptor deficient; MCMV, murine cytomegalovirus; pDC, plasmacytoid dendritic cell; TLR, Toll-like receptor.

DCs are potent APCs that initiate T cell-dependent immune responses (1). After exposure to a variety of inflammatory stimuli, including ligands for Toll-like receptors (TLRs; reference 2), DCs undergo phenotypic and functional changes that characterize their transition from immature to mature DCs exhibiting a strong capability to initiate an immune response. A complex modulation of chemokine responsiveness and production is responsible for mature/activated DC migration from the peripheral tissues into the T cell areas of secondary lymphoid organs where DCs exert their APC functions (3, 4).

DC subpopulations are characterized by expression of different surface markers and ability to produce cytokines that modulate both innate resistance and adaptive immune response (5). In humans, CD11c$^-$ IL-3R^{hi} plasmacytoid DCs (pDCs) differ from CD11c$^+$ conventional DCs (cDCs) in being uniquely able to produce high levels of IFN-α in response to virus stimulation (6, 7) or to oligodeoxynucleotides containing unmethylated CG motifs (CpG-ODN; reference 8). In the mouse, pDCs are CD11c^{low} B220^{high} Ly6C^{high} cells exhibiting plasmacytoid morphology and able to produce high level of IFN-α on exposure to several viruses or to CpG-ODN (9–11). Mouse CD11c^{high} cDCs have been further subdivided in subsets (5). The nature of the T cell response on presentation of antigen by DCs is dependent on the subpopulation of DCs involved, the antigen dose, the cytokine environment, and the stage of maturation of presenting DCs (12–14). DC subtypes also link acquired and innate resistance responses (15), with cDCs activating both B cells (16) and NK cells (17), and pDCs producing large amounts of type I IFN in response to viruses as well as playing an essential role in activating NK cells to kill virus-infected cells (18).

The pattern of TLR expression in different DC types and their interaction with specific pathogen-derived ligands regulate cytokine production and direct the type of immune response (13, 19). The role of specific TLR in mediating type I IFN production in response to viral stimulation (in particular TLR3 and -4 in cDCs and TLR7 and -9 in pDCs) has recently been demonstrated (20–23). Type I IFNs (IFN-α, -β, or -ω) are cytokines exhibiting antiviral activity as well as a variety of other biological effects on macrophage function,

The online version of this article contains supplemental material.

NK cell activity, Th1 differentiation, CTL generation and activity, and T cell survival and proliferation. They play a central role in host resistance to viral or microbial infections (24, 25) and are often considered important components linking innate and adaptive immunity (24–26).

It has been suggested that type I IFN promotes and may be necessary for human and mouse DC maturation, including up-regulation of costimulatory molecules and ability to stimulate T cells. A role for type I IFN in mouse DC activation after viral or TLR-mediated stimulation has been proposed, largely on the basis of studies with DCs derived in vitro from BM cells in the presence of GM-CSF (BM-DCs; references 27, 28) that did not provide information on physiological DC subsets and failed to mimic the in vivo situation in which high amounts of type I IFN are produced. In particular, BM-DCs did not contain pDCs, the major type I IFN producing cells in vivo in response to viruses and certain TLR-ligands. Although polyinosinic–polycytidylic acid induces high IFN-β production in cells other than pDCs, including BM-DCs, LPS and CpG-ODN induce only low levels of IFN-β in BM-DCs (28). In the present study, we demonstrate that mouse pDC and cDC subsets differ in type I IFN requirements for in vivo activation and migration induced by treatment with TLR ligands.

RESULTS

Type I IFN production in vivo after TLR ligand injection

We first investigated the ability of TLR4, -7, and -9 ligands to induce type I IFN secretion in vivo. Both IFN-α (as detected by an ELISA measuring the mouse IFN-α1, -α4, -α5, -α6, and -α9) and type I IFN (as detected by biological antiviral assay, in the presence of neutralizing anti-IFN-γ) were detectable in the serum of resiquimod- or CpG-ODN–treated mice, with a peak at 2 h and 4 h, respectively (Fig. 1 A). No detectable level of IFN-α and very low levels of type I IFN (10 U/ml ±4.6) were detected in the serum of LPS-treated mice only at 2 h after treatment (Fig. 1 A). Mouse pDCs have previously been demonstrated to be the major IFN-α producing cells in vitro in response to CpG-ODN and in vivo after virus infection (9). We investigated the nature of the type I IFN–producing cells in vivo in response to TLR7 and TLR9 ligands. After both resiquimod and CpG-ODN treatment, only 120G8^{+}CD11c^{low} pDCs expressed intracellular IFN-α (6.1% and 8.7% positive cells, respectively; Fig. 1 B), whereas no staining could be detected in CD11c^{high} cDCs (Fig. 1 B), B cells, T cells, macrophages, or NK cells (unpublished data). To investigate the regulation by type I IFN on its own production in vivo, WT and IFNAR$^{-/-}$ mice were treated with TLR4, -7, and -9 ligands. In IFNAR$^{-/-}$ mice, both IFN-α and type I IFN production in vivo in response to CpG-ODN were almost completely abolished 6 h after treatment (Fig. 1 C). In contrast, resiquimod-induced type I IFN production was similar in WT and IFNAR$^{-/-}$ mice 2 h after the treatment, although IFN-α secretion was decreased ∼50% in the latter

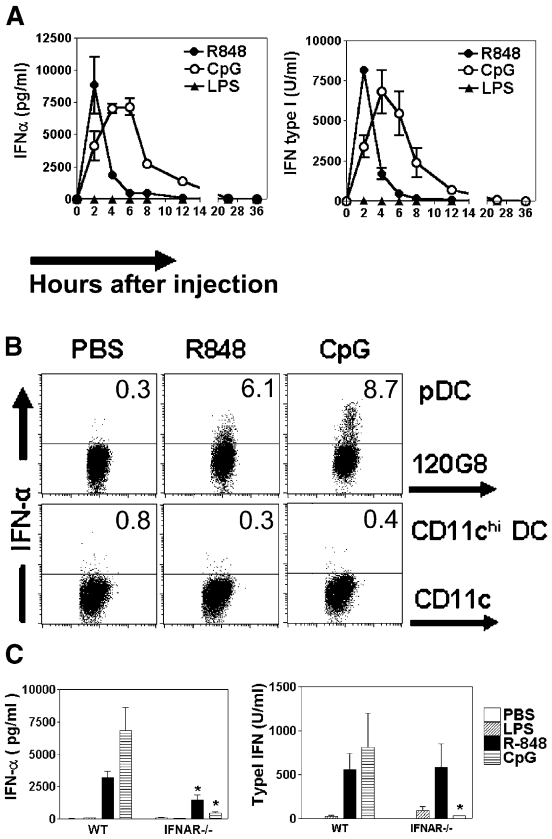

Figure 1. In vivo production of type I IFN in response to TLR ligands. (A) Sera from 129Sv WT mice were collected at different time point after LPS, resiquimod (R-848), or CpG-ODN treatment and titrated for IFN-α by ELISA and type I IFN by biological assay. The sera of mice injected with DOTAP alone were negative for IFN-α and type I IFN. Mean cytokine concentration (± SEM) of three mice per group is shown (two independent experiments giving similar results). (B) Spleen cells from 129Sv WT mice were collected 3 h after PBS or CpG-ODN injection, or 1 h after resiquimod injection and stained, as described in Materials and methods. pDC were gated as 120G8^{+}CD11c^{low} cells. CD11c^{high} DC were gated as 120G8^{-}CD11c^{high} cells. Dot plots shown for each staining are representative of at least three determinations in two separate experiments. (C) Sera from 129Sv WT mice or IFNAR$^{-/-}$ mice were collected 2 h after PBS, LPS, or resiquimod treatment and 6 h after CpG-ODN treatment and titrated for IFN-α by ELISA and IFN type I by biological assay. Mean cytokine concentration (± SEM) of 6–16 mice per group is shown (two to five independent experiments giving similar results). *, $P < 0.01$, compared with WT mice.

(Fig. 1 C). A mixture of neutralizing rabbit anti-IFN-α and anti-IFN-β polyclonal antibody (pAb) abolished more than 90% of the antiviral activity measured in the serum of resiquimod- and CpG-treated mice (unpublished data), indicating that the antiviral activity was mostly caused by the presence of IFN-β and IFN-α. LPS in both WT and IFNAR$^{-/-}$ mice induced no detectable IFN-α and very low levels of type I IFN (Fig. 1 C), and LPS-induced type I IFN antiviral activity was completely blocked by a neutralizing rabbit anti-IFN-β pAb (unpublished data). Thus, TLR7-

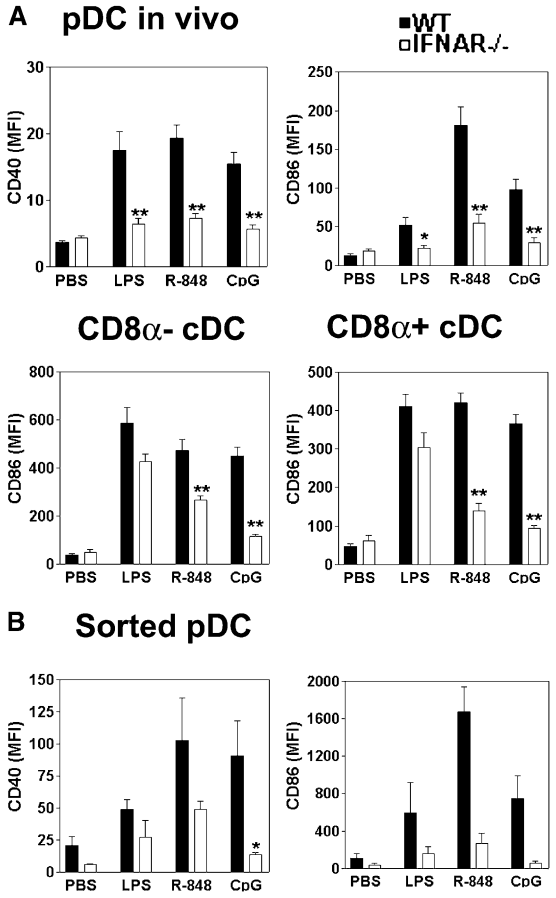

Figure 2. Mouse DC subset activation in response to TLR ligands. (A) Spleen cells from 129Sv WT mice or IFNAR$^{-/-}$ mice, treated with PBS, LPS, resiquimod (R-848), or CpG-ODN, were collected 6 h after treatment and stained as described in Materials and methods. CD40 (left panels) and CD86 (right panels) expression on 120G8^{+}CD11c^{lo} pDC (upper panels), only CD86 on CD8^{-} cDC (lower right panel), and CD8^{+} cDC (lower left panel) were analyzed. Mean fluorescence intensity (MFI) ± SEM of six mice per group (two independent experiments giving similar results) is shown. (B) Sorted 120G8^{+}CD11c^{low} pDC were isolated from 129Sv WT mice or IFNAR$^{-/-}$ mice and stimulated with medium, LPS, resiquimod, or CpG-ODN as described in Materials and methods. MFI ± SEM of CD40 (left panels) and CD86 (right panels) expression is shown for three independent experiments. *, $P < 0.05$; **, $P < 0.01$, compared with WT mice.

and TLR9-induced type I IFN and IFN-α secretion are differentially regulated by type I IFN in vivo.

Role of type I IFN in TLR-mediated activation of DC subsets

We next investigated the role of type I IFN signaling in TLR-mediated in vivo activation of DC subsets. Activation of DC subsets was studied 6 h after injection of TLR ligands in both WT and IFNAR$^{-/-}$ mice. pDCs freshly isolated from untreated WT and IFNAR$^{-/-}$ mice had similar levels of CD40 and CD86 expression (Fig. 2 A). 120G8^{+} pDCs from WT mice up-regulated both CD40 and CD86 expression after LPS, resiquimod, or CpG-ODN treatment in vivo. This up-regulation was absent or much reduced in pDCs from IFNAR$^{-/-}$ mice (Fig. 2 A).

In response to LPS, resiquimod, or CpG-ODN treatment in vivo, both CD8α^{-} CD11c^{high} and CD8α^{+} CD11c^{high} subsets of cDCs from WT mice modestly up-regulated CD40 (unpublished data) and strongly up-regulated CD86 (Fig. 2 A). However, both cDC subsets from IFNAR$^{-/-}$ mice failed to up-regulate CD86 after CpG-ODN stimulation in vivo, whereas LPS induced a comparable increase of CD86 expression level in both WT and IFNAR$^{-/-}$ mice (Fig. 2 A). In response to resiquimod in vivo, the increase in CD86 expression was negligible in the CD8α^{+} cDCs from IFNAR$^{-/-}$ mice and was significantly lower in CD8α^{-} cDCs from IFNAR$^{-/-}$ mice than in CD8α^{+} cDCs and CD8α^{-} cDCs from WT mice (Fig. 2 A).

To elucidate the role of type I IFN secretion in TLR-mediated activation of purified pDCs, spleen 120G8^{+} CD11c^{low} pDCs were isolated by fluorescence-activated cell sorting from WT 129 mice and IFNAR$^{-/-}$ mice. The purified pDCs were then cultured in vitro for 20 h in the presence or absence of LPS, resiquimod, or CpG-ODN. Although isolated pDCs from WT mice slightly up-regulated CD40 and CD86 after 18 h culture in the absence of TLR ligands (unpublished data and Fig. 2, A and B), the cultured pDCs from IFNAR$^{-/-}$ mice exhibited a lower level of CD40 and CD86 expression than those from WT mice (Fig. 2 B). pDCs from WT mice cultured in the presence of CpG-ODN or resiquimod, and, to a lower extent, LPS, strongly up-regulated both CD40 and CD86 (Fig. 2 B). In pDCs from IFNAR$^{-/-}$ mice, the up-regulation of CD40 and CD86 in response to CpG-ODN was abolished. In contrast, pDCs from IFNAR$^{-/-}$ mice up-regulated both CD40 and CD86 in response to resiquimod and LPS, although the level of expression was much reduced compared with that observed in pDCs from WT mice.

Migration of spleen DC subsets

In vivo DC activation by microbial products, such as LPS or extracts of *Toxoplasma gondii* and *Leishmania donovani*, has been shown to induce migration of CD11c^{high} cDCs from the marginal zone and outer periarteriolar lymphatic sheaths (PALs) into the T cell area (29, 30). Using the 120G8 mAb that detects an antigen highly expressed on both resting and activated pDCs (31), we have investigated the migration of pDCs within spleen in mice treated with TLR ligands. We have compared it with that of cDCs identified as CD11c^{high}. Because of the low expression of CD11c on pDCs, immunohistochemical staining with anti-CD11c and 120G8 allowed us to distinguish between pDCs and cDCs (31). In untreated mice, 120G8^{+} pDCs were scattered mainly in the T cell area and in the red pulp, although, rarely, pDCs could be detected in the marginal zone (Fig. 3 A). In contrast, CD11c^{high} cDCs were mostly located in the outer PALs and in the marginal zone, with few cDCs detected in the red pulp (Fig. 3 A). At 6 h after treatment with LPS, spleen

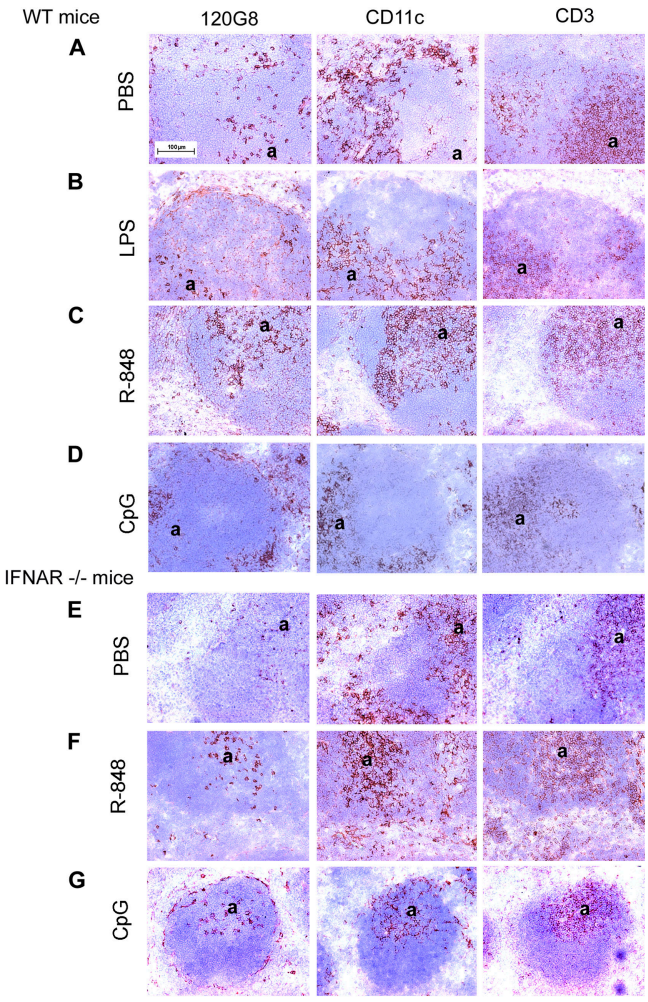

Figure 3. Spleen dendritic cells localization after TLR treatment. (A–D) Spleens from 129Sv WT mice were collected 6 h after treatment with (A) PBS, (B) LPS, (C) resiquimod (R-848), or (D) CpG-ODN. (E–G) Spleens from IFNAR$^{-/-}$ mice were collected 6 h after treatment with (E) PBS, (F) resiquimod, or (G) CpG-ODN. Spleen serial sections were obtained and stained with 120G8 (pDC, left panels), anti-CD11c (cDC, middle panels) or anti-CD3ε (T cells, right panels) Abs as described in Materials and methods. One representative staining out of three mice per group is shown (two independent stainings). a, arteriol.

pDCs remained scattered in the T cell area and in the red pulp (Fig. 3 B). At 6 h after treatment with CpG-ODN and resiquimod, although some isolated pDCs could still be detected in the red pulp, most spleen pDCs formed clusters in the marginal zone and in the T cell area (Fig. 3, C and D). Although CpG-ODN treatment induced pDC clusters mostly located in the marginal zone (Fig. 3 D), after resiquimod treatment those clusters were located in the T cell area rather than in the marginal zone, and some isolated pDCs could be detected in the T cell area (Fig. 3 C). Unlike pDCs, cDCs migrated in the inner T cell area in response to all the three TLR ligands tested (Fig. 3, A–D). Enumeration of total number of spleen pDCs revealed that pDC number decreased by approximately one half to one third at 6 h after all TLR treatment. At 24 h after treatment with CpG-ODN or resiquimod, only a minimal recovery of pDC number was observed (Fig. S1, available at http://www.jem.org/cgi/content/full/jem.20041930/DC1).

Role of type I IFN in TLR-mediated spleen pDC migration

We next addressed the question whether type I IFN would play a role in spleen pDC migration in response to TLR7 and -9 ligands. No change in spleen pDC localization was observed 6 h after injection of recombinant mouse IFN-α (unpublished data). As previously reported (31), the intensity of 120G8 staining was lower in IFNAR$^{-/-}$ mice than in WT mice. In untreated IFNAR$^{-/-}$ mice, scattered spleen 120G8^{+} pDCs were detected both in the T cell area and in the red pulp, as in normal WT mice (Fig. 3 E). Unlike in WT mice, spleen 120G8^{+} pDC did not form clusters in CpG-ODN- or resiquimod-treated IFNAR$^{-/-}$ mice. Scattered pDCs were found both in the T cell area and in the red pulp. Strikingly, although some pDC were found in the marginal zone of CpG-ODN–treated IFNAR$^{-/-}$ mice, they were mostly located in the T cell area, unlike in WT mice (Fig. 3, F and G). In contrast, CD11c^{high} cDCs migrated to the T cell area in IFNAR$^{-/-}$ mice treated with CpG-ODN or resiquimod, similarly to WT mice (Fig. 3, F and G).

Kinetics of pDC in situ migration in response to CpG-ODN and resiquimod

To characterize spleen pDC migration in response to TLR7- and TLR9-mediated activation further, double immunohistofluorescent staining with 120G8 mAb and anti-CD3, anti-CD11c, or anti-CD19 mAb was performed on spleen sections from PBS-, CpG-ODN–, and resiquimod-treated mice, at 6 h and 24 h after treatment (Fig. 4). In untreated mice, as described in Fig. 3 A, 120G8^{+} pDCs were scattered in the T cell area and colocalized with cDCs only in the outer PALs. At 2 h and 4 h after resiquimod treatment, no pDC clusters were detected, and 120G8^{+} pDCs were distributed both in the red pulp and the T cell area, with a pattern of localization similar to that in spleens from untreated mice (unpublished data). At 6 h after resiquimod treatment, 120G8^{+} pDCs formed clusters in the T cell area (Fig. 4 B), and cDCs were distributed throughout the entire T cell area (Fig. 4 B). However, although an analysis of many sections showed that at 6 h the clusters of pDCs were predominant in the outer T cell area, at 24 h most 120G8^{+} pDCs were closer to the central artery (Fig. 4 C). At 6 h after CpG-ODN treatment, clusters of 120G8^{+} pDCs were localized in the marginal zone (as identified by staining with ER-TR9 mAb, unpublished data) but not in the T cell area identified by anti-CD3 staining (Fig. 4 D). CD11c^{hgh} cDCs did not colocalize with 120G8^{+} pDCs at 6 h after CpG-ODN treatment (Fig. 4 D). In contrast, at 24 h after treatment, the clusters of 120G8^{+} pDCs were localized inside the T cell area and colocalized with CD11c^{high} cDCs (Fig. 4 E).

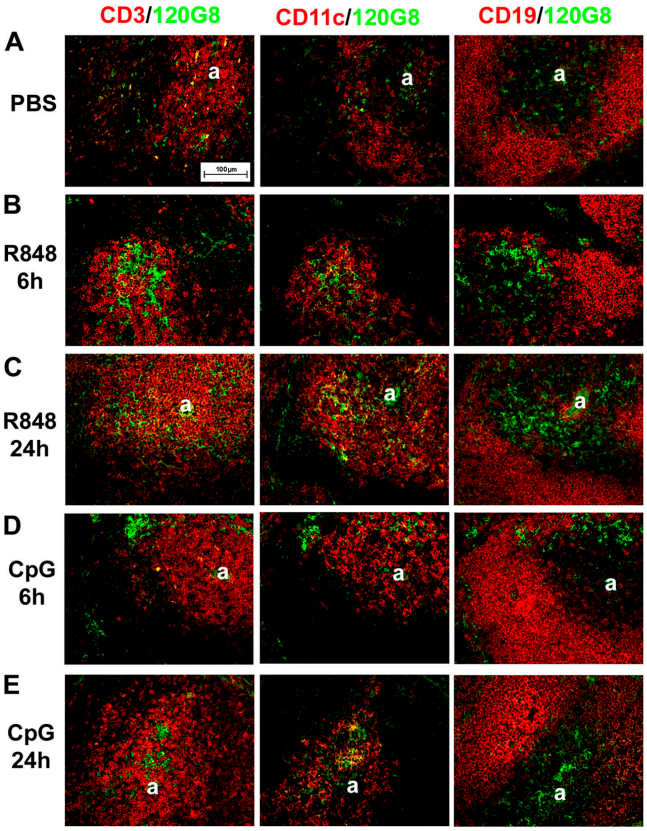

Figure 4. Kinetics of spleen pDC in situ migration after resiquimod (R-848) or CpG-ODN treatment. Spleen from 129Sv mice were collected at 6 h or 24 h after (A) PBS, (B, C) R-848, or (D, E) CpG-ODN treatment, as described in Materials and methods. Spleen serial sections were obtained and costained with 120G8 in green and in red: anti-CD3ε (left panels), anti-CD11c (middle panels), or anti-CD19 (right panels) Abs, as described in Materials and methods. Overlaid pictures of the two fluorescences on identical sections are shown, for one representative mouse of three per group. a, arteriol.

Possible involvement of CXCR3 and CCR7 in pDC migration pattern

Migration of pDCs into inflamed lymph node has been suggested to be initially mediated by CXCR4 and CXCR3 ligands (32). Chemokines such as CCR7 ligands also play a major role in migration of activated DCs from peripheral tissue into lymphoid organs (33). We investigated the ability of in vivo CpG-ODN–activated spleen pDCs to migrate in vitro in response to CXCR3 , CXCR4, or CCR7 ligands. Mice were injected intravenously with CpG-ODN, and spleens were collected at 0, 2, 6, and 24 h after treatment. pDCs from untreated mice migrated in response to CXCR4 ligands (CXCL12), CXCR3 ligands (CXCL9), and CCR7 ligands (CCL19, CCL21), but not in response to CCR6 ligands (CCL20) (Fig. 5 A). The migration index of pDCs in response to CXCL12 remained constant at the different time points after in vivo activation with CpG-ODN. The pDC migration in vitro in response to CXCL9 was decreased as early as 2 h after CpG-ODN injection, whereas pDC ability to migrate in vitro in response to both CCR7 ligands CCL19 and CCL21 was up-regulated 6 h after CpG-ODN treatment in vivo. The role of type I IFN in migratory response of activated pDCs to CXCL9 and CCL21 was further investigated. The migration index of pDCs in response to CXCL9 was slightly higher in untreated IFNAR$^{-/-}$ mice than in WT mice, whereas in vitro CCL21 induced a comparable migration of untreated pDCs in WT and IFNAR$^{-/-}$ mice. At 6 h after CpG-ODN treatment, the capacity of IFNAR$^{-/-}$ pDCs to migrate in response to CXCL9 was not significantly reduced compared with PBS treatment. In contrast, the ability of IFNAR$^{-/-}$ pDCs to migrate in vitro in response to CCL21 was up-regulated at 6 h after CpG-ODN treatment, although to a lower extent than in WT mice (Fig. 5 B).

The expression and localization of both CXCR3 and CCR7 ligands were investigated in WT and IFNAR$^{-/-}$ mice. Although no CCL21 could be detected in WT and IFNAR$^{-/-}$ mice serum at 2 and 6 h after CpG-ODN treatment (unpublished data), cells positive for CCL21 staining were detected in the spleen T cell area of both untreated and CpG-ODN–treated WT and IFNAR$^{-/-}$ mice (Fig. 5 C). Similar observations were obtained in resiquimod-treated WT mice (Fig. 5 C). Both CXCL9 and CXCL10 were detected in the serum of CpG-ODN–treated mice 6 h after injection (5.45 ng/ml ±1.9 and 2.04 ng/ml ±0.9, respectively). In resiquimod-treated mice, both chemokines were already secreted at 2 h after injection and were minimally decreased at 6 h after injection (7.4 ng/ml ±0.3 and 2.1 ng/ml ±0.38, respectively). Secretion of both chemokines was much reduced in the serum of CpG-treated IFNAR$^{-/-}$ mice compared with WT mice (CXCL9: 0.27 ng/ml ±0.5; CXCL10: 0 ng/ml in IFNAR$^{-/-}$ mice; detection limit = 0.1 ng/ml). No staining using anti-CXCL10 goat pAb could be observed in spleens from treated and untreated WT and IFNAR$^{-/-}$ mice (unpublished data). Using anti-CXCL9 goat pAb, no specific staining could be detected in spleens from untreated WT mice. In contrast, at 6 h after CpG-ODN and resiquimod injection, cells brightly positive for CXCL9 intracellular expression were observed in the red pulp (Fig. 5 C). Some additional CXCL9^{+} cells were detected in the spleen T cell area of resiquimod-treated WT mice (Fig. 5 C). Spleens of CpG-treated IFNAR$^{-/-}$ mice displayed a pattern of CXCL9 staining similar to that of WT mice (Fig. 5 C), although the staining intensity was lower.

Mouse pDC localize in the marginal zone after virus stimulation

To investigate whether spleen pDCs display a pattern of migration after virus infection similar to that seen with TLR treatment, mice were injected i.p. with infectious murine cytomegalovirus (MCMV). Viral infection and TLR ligand treatment induced different kinetics of cytokine and chemokine production. It has been reported previously that the peak of type I IFN secretion, detected at 36 h after in vivo MCMV

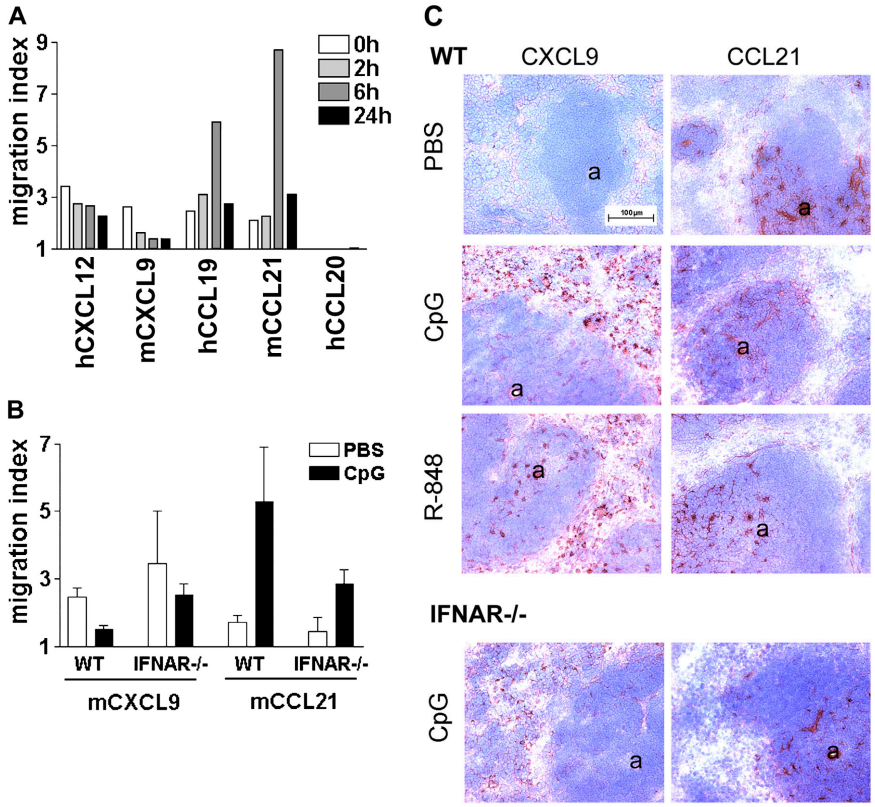

Figure 5. Role of CCL21 and CXCL9 chemokines in migration of CpG-activated mouse pDC in the spleen. (A) Spleens from 129Sv mice were isolated 0 h, 2 h, 6 h, and 24 h after CpG-ODN in vivo treatment. Response of activated spleen pDC to various chemokines was studied in Transwell (Corning, Inc.) migration assay. Results are expressed as a migration index (number of migrating cells in chemokine/number of migrating cells in medium). One representative experiment three is shown. (B) Spleens from 129Sv WT and IFNAR$^{-/-}$ mice were isolated 6 h after PBS or CpG-ODN in vivo treatment. Response of activated spleen pDC to CXCL9 and CCL21 was studied in Transwell migration assay. Mean migration index from at least three independent experiments is shown. (C) Spleens from 129Sv WT and IFNAR$^{-/-}$ mice were collected 6 h after treatment with PBS, CpG-ODN, or resiquimod. Spleen sections were obtained and stained with anti-CXCL9 (left panels) or -CCL21 (right panels) Abs as described in Materials and methods. One representative staining out of three mice per group is shown. a, arteriol.

infection, is dependent on the presence of pDCs (9). Thus, we investigated the pattern of pDC migration at this crucial time point. Thirty-six hours after MCMV infection, clusters of 120G8$^+$ pDCs were observed in the marginal zone of the spleen, whereas CD11c^{high} cDCs redistributed to the T cell area (Fig. 6, A and B). To confirm that 120G8$^+$ pDC were type I IFN–producing cells after MCMV infection, we performed double staining with 120G8 mAb and rat anti–mouse IFN-α mAb on spleen sections from 1.5-d MCMV-infected mice. Some nonspecific staining could be detected with anti-IFN-α antibody, on endothelial cells from both uninfected and infected mice (unpublished data). However, positive and strong immunostaining for IFN-α was detected in the marginal zone of MCMV infected mice only. Cells positive for IFN-α were also positive for 120G8 staining. In contrast, some 120G8$^+$ pDC clusters did not stain for IFN-α (Fig. 6 C).

DISCUSSION

pDCs and cDCs express different TLR (8, 13, 34). In the mouse, it has been reported that although TLR9 is expressed on pDCs and cDCs, TLR7 is present on pDCs and CD8α$^-$ CD11c^{high} cDCs but is absent on CD8α$^+$CD11c^{high} cDCs (19). Although TLR4 is highly expressed on BM-derived myeloid DCs, it is expressed only at a low level on spleen cDCs and pDCs (13). Data on TLR expression and TLR-mediated activation of in vitro derived DCs and ex vivo isolated DC subsets have often been used to speculate on the ability of natural TLR ligands to activate DC subsets differentially during infections. However, our data indicate that DC subsets are equally activated with in vivo treatment with TLR ligands such as LPS, CpG-ODN, or resiquimod. Particularly striking is the in vivo activation by resiquimod of CD8α$^+$CD11c^{high} DCs that do not express TLR7 and that are not activated in vitro by TLR7 ligands (19). Indeed, to understand in vivo DC activation during infections or on treatment with TLR ligands, cellular and humoral interactions should be considered not only among the DC subsets, but also with other immune and nonimmune cells responding to TLR ligands.

It has been shown that DCs derived in vitro in the presence of GM-CSF or ex vivo isolated total spleen DCs spon-

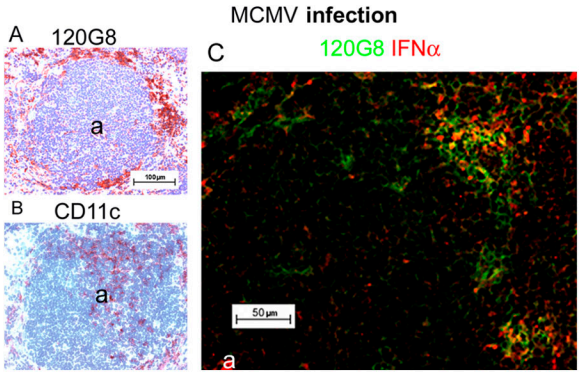

Figure 6. Dendritic cells localization in mouse spleens after MCMV infection. Spleens from 129Sv WT mice were collected 1.5 d after viral infection with MCMV. Spleen sections were stained with (A) 120G8 (pDC) or (B) anti-CD11c (cDC) Abs as described in Materials and methods. (C) Spleen sections were costained with 120G8 in green and anti-IFNα mAb in red, as described in Materials and methods. Overlaid pictures of the two fluorescences on identical sections are shown, for one representative staining out of three mice per group. a, arteriol.

taneously secrete type I IFN that acts in an autocrine manner to promote their functional and phenotypic maturation (35, 36). Consistent with those data, we observed that pDCs (Fig. 2, A and C) and, to a lesser extent, cDCs from IFNAR$^{-/-}$ mice (unpublished data) in neutral culture conditions underwent a lower maturation than DCs from control WT mice, although no type I IFN secretion was detected under those conditions. DCs freshly isolated from IFNAR$^{-/-}$ and WT mice expressed comparable low levels of maturation/activation markers (Fig. 2). No significant differences in DC frequency could be detected in various organs from WT and IFNAR$^{-/-}$ mice (unpublished data), suggesting that, in noninflammatory conditions, the in vivo development of both pDCs and cDCs does not require endogenous type I IFN.

The in vivo activation of pDCs in response to TLR ligands, as analyzed by up-regulation of expression of CD40 and CD86, was profoundly depressed in IFNAR$^{-/-}$ mice. In contrast, type I IFN played a major role in the activation of both subsets of cDCs as analyzed by up-regulation of CD86, but only after treatment with CpG-ODN and, in part, with resiquimod. Indeed, in vivo, LPS-mediated CD86 expression on cDCs was not dependent on type I IFN signaling. Up-regulation of CD40 in vivo in cDCs was modest, and a possible role for type I IFN could not be reliably evaluated.

Type I IFN played a major role in CpG-ODN–mediated but not in LPS- or resiquimod-mediated in vitro activation of sorted pDCs. This finding is consistent with the observation that sorted pDCs produced high amounts of IFN-α and type I IFN in vitro in response to CpG-ODN, but not in response to LPS, and produced very low levels in response to resiquimod (unpublished data), although in vivo pDCs produced high levels of IFN-α after resiquimod treatment. Our unpublished observations on sorted cDC subsets indicated that in response to resiquimod and CpG-ODN in vitro, these cells did not produce type I IFN, and that their activation was type I IFN independent. However, as previously reported for LPS-induced CD40 expression in BM-DCs (27, 28), LPS-mediated CD11b^{+} cDC activation in vitro was reduced in IFNAR$^{-/-}$ mice, although LPS-activated sorted cDCs secreted no detectable level of type I IFN (unpublished data). Taken together, our results suggest an intrinsic dependence of pDCs on type I IFN for optimal activation in vivo in response to several TLR ligands, and only a partial and indirect dependence of cDCs, mostly observed under in vivo conditions, that results in high systemic type I IFN secretion by pDCs.

The migration pattern of activated cDCs in spleen has been extensively studied, but little or no information is available for pDCs. In the spleen of untreated mice, as we previously described, pDCs are dispersed through the T cell area but are also scattered in the marginal zone and red pulp (31). cDCs, unlike pDCs, are mostly localized in the marginal zone bridging channel, and only few interdigitating DCs are present in the T cell zone (37). In the spleen of CpG-ODN– or resiquimod-treated mice, CD11c^{high} cDCs, similar to previous descriptions of response to LPS or *T. gondii* extracts (30), migrated from the bridging channel into the T cell area, whereas pDCs formed clusters and displayed very specific changes in anatomic localization. After resiquimod treatment, the clusters of pDCs were present in the T cell zone, primarily in the outer PALs at 6 h after treatment, but by 24 h pDCs were also present in the inner PALs. At 24 h after treatment with CpG-ODN, pDC clusters were also observed in the T cell zone, but at 6 h, the pDC clusters were mostly found in the marginal zone, separated from the majority of T cells and cDCs. Thus, unlike cDCs, pDCs are not in contact with T cells soon after CpG-ODN treatment, but later they partially colocalized with T cells and cDCs. Whether the late localization of pDCs in the T cell area reflects a migration of the pDCs that clustered in the marginal zone at earlier times or the entry of new pDCs in the inflamed spleen via the central artery remains to be investigated. Indeed, although the total number of spleen pDCs decreased after TLR treatment, this reduction does not exclude the possibility that, although activated pDCs undergo massive cell death, some newly activated pDCs might enter the T cell area.

In mice exposed to either infectious MCMV (Fig. 6) or inactivated HSV (unpublished data), pDCs migrated and aggregated in the marginal zone, much as observed at 6 h after CpG-ODN treatment. At 36 h after infection, IFN-α–producing cells colocalized in the marginal zone with clusters of pDCs, although some clusters of activated pDCs did not produce IFN-α. This lack of IFN-α could result from different kinetics between activation, migration, clustering, and IFN production. At later time points, a dramatic decrease in pDC frequency, as well as the lytic properties of MCMV infection in vivo, prevented us from following the fate of pDC

clusters (unpublished data). These data are consistent with an early report demonstrating that after HSV-1 stimulation, IFN-producing cells, now identified as pDCs, could be detected in the spleen marginal zone (38).

Human and mouse resting pDCs previously have been shown to respond spontaneously to CXCL12, a CXCR4 ligand found on high endothelial venules in human tonsils or lymph nodes (32, 39). Human pDCs do not migrate in response to CXCR3 ligands in vitro, but exposure or pretreatment to inflammatory CXCR3 ligands drastically enhances their ability to migrate in response to the constitutive chemokine CXCL12 (32, 40). This feature has been shown to be important both for pDC migration to inflamed tissues and for pDC transmigration through high endothelial venules into inflamed lymph nodes (41). In addition, up-regulation of CCR7 and responsiveness to the CCR7 ligands CCL21 and CCL19 has been shown to be involved in migration of cDCs from peripheral tissue to lymphoid organs and from the marginal zone bridging channel into the T cell area where these chemokines are produced and are also responsible for attraction of naive T cells. In accordance with their respective TLR expression, human blood $CD11c^+$ myeloid DCs up-regulate CCR7 and down-regulate CCR5 in response to LPS but not in response to CpG-ODN, whereas human blood pDCs up-regulate CCR7 and down-regulate CXCR3 in response to CpG-ODN but not in response to LPS (34). We now show that mouse spleen pDCs, 6 h after in vivo treatment with CpG-ODN, acquire the ability to migrate in response to the CCR7 ligand CCL21. We also demonstrate that the capacity of spleen pDCs to migrate in response to the CXCR3 ligand CXCL9 decreases starting at 2 h after in vivo treatment with CpG-ODN, as previously reported in vitro for mouse BM-derived pDCs, consistent with the down-regulation of CXCR3 expression upon ligation with its specific ligand (32). CXCL9 is produced after CpG-ODN treatment in the red pulp and marginal zone, but not in the PALs. Taken together, these data suggest that the initial migration and clustering of mouse pDCs after CpG-ODN treatment in the marginal zone results from their ability to migrate toward a gradient of constitutive CXCL12 and of CXCR3 ligands such as CXCL9 induced by IFN and other proinflammatory cytokines in the red pulp. At later time points, when the response to CXCR3 ligands decreases and is followed by an increase in the response to CCR7 ligands, pDCs, like cDCs, may migrate or accumulate into the T cell area where CCL21 is constitutively produced. It is not known why early pDC clustering in the marginal zone is not observed in response to treatment with the TLR7 ligand, resiquimod. resiquimod and CpG-ODN treatment induced similar levels of both CXCR3 ligands, CXCL9 and CXCL10, in the serum of treated mice, as well as highly positive CXCL9 cells located in the spleen red pulp. However, the very different kinetics of cytokine and chemokine production, as well as pDC activation in response to TLR7 and -9 ligands on one hand, and the presence of $CXCL9^+$ cells in the spleen T cell area of resiquimod-treated mice on the other hand, may provide some explanations for this difference. Thus, the overall migration pattern of pDCs after TLR treatment seems to involve a complex interplay between chemokine receptor expression by pDCs and chemokine secretion (kinetic and pattern) by both pDCs and non-pDCs.

pDCs and cDCs differentially require type I IFN for in situ migration in response to TLR ligands. Indeed, neither aggregation nor migration of pDCs outside the T cell area was observed in $IFNAR^{-/-}$ mice in response to CpG-ODN. After resiquimod treatment, no aggregation of pDCs in the T cell area could be observed in $IFNAR^{-/-}$ mice. However, because resiquimod-activated pDCs are mostly located in the T cell area in both WT and $IFNAR^{-/-}$ mice, it is difficult to reach conclusions about the role of type I IFN in TLR7-induced pDC migration. In contrast, cDCs still displayed the characteristic migration in the T cell area in $IFNAR^{-/-}$ mice.

Previous studies have shown that type I IFN signaling is required for maturation but not for up-regulation of CCR7 on BM-DC or migration of cDCs in response to Newcastle Disease Virus and polyinosinic–polycytidylic acid in vivo (27). Similarly, pDCs from CpG-ODN–treated $IFNAR^{-/-}$ mice still up-regulated their responsiveness to CCR7 ligand CCL21, although to a lesser extent than in WT mice. Although some CXCL9-producing cells could still be detected in the spleen of CpG-treated $IFNAR^{-/-}$ mice, in vivo secretion of both CXCL10 and CXCL9 was much decreased in the serum of CpG-treated $IFNAR^{-/-}$ mice, compared with WT mice. Moreover, because CXCR3 expression is down-regulated on ligation with CXCR3 ligands (32), a lower secretion of type I IFN–regulated CXCR3 ligands in $IFNAR^{-/-}$ mice may explain both the higher level of CXCR3 expression in resting pDCs and the absence of CXCR3 down-regulation after CpG-treatment. Thus, while cDCs need to up-regulate CCR7 to migrate in response to CCR7 ligands, the expression of which is constitutive and type I IFN independent. In contrast, the early pDC clustering and migration may depend on the intrinsic ability of these cells to migrate in response to a combined gradient of constitutively expressed CXCL12 and type I IFN–induced CXCL9 and CXCL10 in inflammatory conditions. The need for induction of IFN-dependent inflammatory chemokines in the early hours of response, as well as the fact that, unlike cDCs, in pDCs the maturation and functional activation, including up-regulation of CCR7, is reduced in the absence of type I IFN, could in part explain the different type I IFN requirements for in situ migration of cDCs and pDCs.

The localization of the pDCs in different spleen compartments during the inflammatory response may be important for their ability to affect the response by secreting cytokine (e.g., type I IFN) or to interact with T cells directly. Interestingly, in response to viruses, TLR ligands, or

CD40L, pDCs produce CXCL9 and CXCL10 and, through their production of type I IFN, can recruit immature cDCs to produce high amounts of inflammatory chemokines, which may exert a chemotactic effect on $CD8^+$ effector T cells and NK cells (32, 42, 43). One striking characteristic of in vivo pDC activation is their tight clustering. It remains to be determined whether the autocrine pDC production of inflammatory chemokines during activation plays a role in inducing their aggregation, possibly in addition of cross-activation via type I IFN and activation of adhesion molecules.

MATERIALS AND METHODS

Mice, culture medium, and antibodies. Specific pathogen-free female 129/SvPas mice, 6–10 wk of age, were purchased from Charles River. $IFNAR^{-/-}$ mice (A129 strain, mice deficient for the β1 chain of type I IFN receptor) were purchased from B&K Universal Ltd. and bred by Charles River. All mice experiments were performed following protocols approved by the institutional animal committee and in accordance with European Economic Community Council Directive 86/609 as well as institutional animal care and use guidelines.

Primary cells were cultured in complete medium: RPMI 1640 (Life Technologies) supplemented with 10% (vol/vol) heat-inactivated FCS (Life Technologies), 2 mM L-glutamine (Life Technologies), 80 μg/ml gentamycine (Schering-Plough Corporation), 10 mM Hepes (Life Technologies), and 50 μM β_2-mercaptoethanol (Sigma-Aldrich), at 37°C in 5% CO_2. All antibodies were from BD Biosciences unless otherwise specified.

In vivo treatment. For in vivo treatment with TLR ligands, mice were anesthetized and injected i.v. in the retro-orbital vein with 200 μl of PBS (Life Technologies), LPS (5 μg in 200 μl of PBS, Sigma-Aldrich), resiquimod (R-848, 5 μg in 200 μl of PBS; Invitrogen), or CpG-ODN preparation. This preparation consisted of 5 μg of CpG-ODN (TCA TTG GAA AAC GTT CTT CGG GGC G, phosphorothioate-modified, from MWG Biotech AG) mixed with 30 μl of a cationic liposome preparation (DOTAP; F. Hoffmann-La Roche Ltd.) and 170 μl PBS in a polystyrene tube. The preparation was injected using a glass syringe. MCMV infections were initiated on day zero by intraperitoneal injection of 5×10^4 plaque-forming units of salivary gland–extracted MCMV, Smith strain. For all in vivo treatment, at the indicated time point, mice were killed by CO_2 inhalation, and spleens were collected for further analysis. If isolated spleen cells were needed, spleens were crushed in cold PBS supplemented with 5% (vol/vol) heat-inactivated FCS and 0.5 mM EDTA (Sigma-Aldrich) (PBS-FCS-EDTA) and passed through a 25-G needle. RBCs were lysed in NH_4Cl solution (StemCell Technologies, Inc.) for 5 min at 4°C. Spleen DCs were enriched from total spleen cells by positive selection using $CD11c^+$ Microbeads and MiniMacs (Miltenyi Biotec).

For analysis of in vivo cytokine and chemokine production, blood was collected by cardiac puncture at the indicated time point after treatment. Serum was prepared from whole blood by coagulation for 30 min at 37°C and centrifugation. Sera were titrated for mouse IFN-α using specific ELISA (PBL Biomedical Laboratories) and for mouse natural type I IFN using a conventional cytopathic effect inhibition bioassay on L-929 cells (CCL-1; American Type Culture Collection), infected with Encephalomyocarditis virus (EMCV, VR-129B, ATCC). All biological assays were performed in the presence of a neutralizing rat anti–mouse IFN-γ mAb (clone R4-6A2), produced in the laboratory. When needed, the assay was performed in the presence of a mixture of neutralizing rabbit anti-IFNα and IFNβ pAb (PBL Biomedical Laboratories). CXCL9, CXCL10, and CCL21 were assayed using specific ELISA (R&D Systems).

Cell sorting and in vitro activation. Isolated spleen cells were incubated for 30 min at 4°C with a mixture of rat anti-CD3 molecular complex (17A2), anti-CD8β (53–5.8), anti-CD19 (1D3), or anti-erythrocyte (TER119). Cells and goat anti–rat IgG-coated Dynabeads (Dynal) were mixed under continuous agitation for 15 min at 4°C. Beads and attached cells were removed using a Dynal magnet. Depleted cells were stained with anti-pDC mAb 120G8-Alexa 488 (31), rat anti-CD8α (53−6.7)-PerCp-Cy5.5, and hamster anti-CD11c (HL-3)-APC for 30 min at 4°C and sorted using a FACSVantage flow cytometer (Becton Dickinson). Sorted cells were washed, resuspended in complete medium, and cultured at 0.5×10^6 cells/ml in 96-well culture plates, for 24 h, in the presence of LPS at 10 μg/ml, resiquimod (R-848) at 10 μg/ml, or CpG-ODN at 10 μg/ml.

FACS analysis. For detection of intracellular IFN-α, 10 μg/ml Brefeldin A (Sigma-Aldrich) was added during the DC enrichment procedure. Cells were first processed with the Fix & Perm kit (BD Biosciences) according to the manufacturer's instructions and then sequentially stained with a mixture of two anti–IFN-α mAbs (F18, Hycult Biotechnology, and RMMA-1, PBL Biomedical Laboratories), goat anti–rat biotin (Jackson ImmunoResearch Laboratories), streptavidin-PE (DakoCytomation) and rat IgG in excess (Sigma-Aldrich). Cells were finally stained for extracellular markers using 120G8-Alexa 488 and hamster anti-CD11c (HL-3)-APC antibodies. For analysis of freshly isolated DC activation, total spleen cells were stained with 120G8-Alexa 488, rat anti-CD40 or CD86-PE, rat anti-CD8α-PerCp-Cy5.5, and hamster anti-CD11c (HL-3)-APC for 30 min at 4°C. For analysis of sorted DC activation, stimulated cells were stained with rat anti-CD40 or CD86-PE. Stained cells were analyzed with a FACScan flow cytometer (Becton Dickinson). Negative controls were performed with corresponding rat or hamster Ig.

Immunohistological staining. After in vivo treatment, mouse spleens were embedded in tissue freezing medium (Jung), flash frozen in liquid nitrogen, and stored at −80°C until further analysis. 5-μm-thick cryosections were fixed in 95% acetone (Sigma-Aldrich) at −20°C for 20 min, dried at room temperature, and stored frozen at −20°C until staining was performed. Serial sections were then rehydrated in PBS. Avidin/biotin tissue content was neutralized using specific kit (Vector Laboratories), and peroxidase tissue content was neutralized using PBS-0.3% H_2O_2 (Sigma-Aldrich). Sections were first incubated with 2% normal mouse serum (DakoCytomation) to eliminate any unspecific antibody binding.

For immunohistochemistry staining, sections were stained sequentially with unlabeled 120G8 rat mAb, anti-CD11c hamster mAb (N418; Endogen), anti-CXCL9, anti-CXCL10, or anti-CCL21 goat pAb (R&D Systems) for 60 min, goat anti–rat, goat anti–hamster, or rabbit anti–goat coupled to biotin (Jackson ImmunoResearch Laboratories) for 60 min, and finally extravidin-peroxidase (Sigma-Aldrich) for 30 min, revealed with AEC (Sigma-Aldrich). Slides were mounted under coverslips with Glycergel (DakoCytomation). For immunofluorescent double staining of DC and T cell populations, sections were stained sequentially with unlabeled rat anti-CD19 for B cells, rat ER-TR9 mAb for marginal zone macrophages (BMA Biomedicals AG), hamster anti-CD3ε for T cells, hamster anti-CD11c (N418) for DC for 60 min, goat anti–rat or anti–hamster coupled to Alexa 594 (Molecular Probes, Inc.) for 60 min, 2% rat serum for 30 min, 120G8 antibody coupled to biotin for 60 min, and finally streptavidin-Alexa 488 (Molecular Probes, Inc.) for 30 min. For immunofluorescent staining of IFN-α producing cells, sections were stained sequentially with unlabeled rat mAb anti-IFN-α (F18, Hycult Biotechnology bv) in PBS-0.1% saponin for 60 min, goat anti–rat coupled to Alexa 594 for 60 min, 2% rat serum for 30 min, rat 120G8 mAb coupled to biotin for 60 min, and finally streptavidin-Alexa 488 for 60 min. Slides were air dried and mounted under coverslips with one drop of Fluoromount G (Electron Microscopy Sciences).

All slides were viewed on an Axioskop epifluorescence microscope (Carl Zeiss MicroImaging, Inc.). Pictures were taken using a MagnaFire Digital Camera (Optronic Laboratories, Inc.). For immunofluorescent double staining, identical sections were photographed for both fluorescent dyes, and pictures were overlaid with ImagePro Express software (Adept Electronic Solutions Pty, Ltd.).

Chemotaxis assay. Migration assays were performed using Costar Transwell (6.5-mm diameter, Corning, Inc.) with 2–3 × 10^5 cells/well. Enriched DC populations were placed for 2 h in inserts with 5-μm pores in the presence or absence of chemokines at 1 μg/ml, and migrating cells were stained with 120G8-Alexa 488 and hamster anti-CD11c (HL-3)-APC. The number of migrating cells was then evaluated with a FACScan flow cytometer (Becton Dickinson). Results are expressed as migration index (ratio number of migrating cells in chemokine/number of migrating cells in medium).

Statistical analysis. Statistical analysis of results was performed using nonparametric Mann-Whitney test. Results are presented as means ± SEM.

Online supplemental material. For analysis of pDC frequency, isolated spleen cells from in vivo–treated mice were first counted by Trypan blue exclusion and stained for 20 min at 4°C with 120G8-Alexa 488, hamster anti-CD11c-APC, and a mixture of anti-CD3ε–, anti-DX5–, and anti-CD19–PE. Stained cells were analyzed with a FACScan flow cytometer (Becton Dickinson). Negative controls were performed with corresponding rat or hamster Ig. Online supplemental material is available at http://www.jem.org/cgi/content/full/jem.20041930/DC1.

We thank I. Durand for FACS sorting assistance.

This work was supported by the Schering-Plough Corporation and the Medical Research Council, United Kingdom.

The authors have no conflicting financial interests.

Submitted: 17 September 2004
Accepted: 23 February 2005

REFERENCES

1. Banchereau, J., and R.M. Steinman. 1998. Dendritic cells and the control of immunity. *Nature*. 392:245–252.
2. Medzhitov, R. 2001. Toll-like receptors and innate immunity. *Nat. Rev. Immunol.* 1:135–145.
3. Forster, R., A. Schubel, D. Breitfeld, E. Kremmer, I. Renner-Muller, E. Wolf, and M. Lipp. 1999. CCR7 coordinates the primary immune response by establishing functional microenvironments in secondary lymphoid organs. *Cell*. 99:23–33.
4. Sallusto, F., and A. Lanzavecchia. 2000. Understanding dendritic cell and T-lymphocyte traffic through the analysis of chemokine receptor expression. *Immunol. Rev.* 177:134–140.
5. Shortman, K., and Y.J. Liu. 2002. Mouse and human dendritic cell subtypes. *Nat. Rev. Immunol.* 2:151–161.
6. Perussia, B., V. Fanning, and G. Trinchieri. 1985. A leukocyte subset bearing HLA-DR antigens is responsible for in vitro alpha interferon production in response to viruses. *Nat. Immun. Cell Growth Regul.* 4:120–137.
7. Siegal, F.P., N. Kadowaki, M. Shodell, P.A. Fitzgerald-Bocarsly, K. Shah, S. Ho, S. Antonenko, and Y.J. Liu. 1999. The nature of the principal type 1 interferon-producing cells in human blood. *Science*. 284:1835–1837.
8. Kadowaki, N., S. Antonenko, and Y.J. Liu. 2001. Distinct CpG DNA and polyinosinic-polycytidylic acid double-stranded rna, respectively, stimulate CD11c(-) type 2 dendritic cell precursors and CD11c(+) dendritic cells to produce type I IFN. *J. Immunol.* 166:2291–2295.
9. Asselin-Paturel, C., A. Boonstra, M. Dalod, I. Durand, N. Yessaad, C. Dezutter-Dambuyant, A. Vicari, O.G. A, C. Biron, F. Briere, and G. Trinchieri. 2001. Mouse type I IFN-producing cells are immature APCs with plasmacytoid morphology. *Nat. Immunol.* 2:1144–1150.
10. Nakano, H., M. Yanagita, and M.D. Gunn. 2001. CD11c(+) B220(+)Gr-1(+) cells in mouse lymph nodes and spleen display characteristics of plasmacytoid dendritic cells. *J. Exp. Med.* 194:1171–1178.
11. Bjorck, P. 2001. Isolation and characterization of plasmacytoid dendritic cells from Flt3 ligand and granulocyte-macrophage colony-stimulating factor-treated mice. *Blood*. 98:3520–3526.
12. Steinman, R.M., S. Turley, I. Mellman, and K. Inaba. 2000. The induction of tolerance by dendritic cells that have captured apoptotic cells. *J. Exp. Med.* 191:411–416.
13. Boonstra, A., C. Asselin-Paturel, M. Gilliet, C. Crain, G. Trinchieri, Y.J. Liu, and O.G. A. 2003. Flexibility of mouse classical and plasmacytoid-derived dendritic cells in directing T helper type 1 and 2 cell development: dependency on antigen dose and differential toll-like receptor ligation. *J. Exp. Med.* 197:101–109.
14. Rissoan, M.C., V. Soumelis, N. Kadowaki, G. Grouard, F. Briere, R. de Waal Malefyt, and Y.J. Liu. 1999. Reciprocal control of T helper cell and dendritic cell differentiation. *Science*. 283:1183–1186.
15. Liu, Y.J. 2001. Dendritic cell subsets and lineages, and their functions in innate and adaptive immunity. *Cell*. 106:259–262.
16. Dubois, B., J.M. Bridon, J. Fayette, C. Barthelemy, J. Banchereau, C. Caux, and F. Briere. 1999. Dendritic cells directly modulate B cell growth and differentiation. *J. Leukoc. Biol.* 66:224–230.
17. Zitvogel, L. 2002. Dendritic and natural killer cells cooperate in the control/switch of innate immunity. *J. Exp. Med.* 195:F9–14.
18. Bandyopadhyay, S., B. Perussia, G. Trinchieri, D.S. Miller, and S.E. Starr. 1986. Requirement for HLA-DR+ accessory cells in natural killing of cytomegalovirus-infected fibroblasts. *J. Exp. Med.* 164:180–195.
19. Edwards, A.D., S.S. Diebold, E.M. Slack, H. Tomizawa, H. Hemmi, T. Kaisho, S. Akira, and C. Reis e Sousa. 2003. Toll-like receptor expression in murine DC subsets: lack of TLR7 expression by CD8 alpha+ DC correlates with unresponsiveness to imidazoquinolines. *Eur. J. Immunol.* 33:827–833.
20. Morrison, L.A. 2004. The Toll of herpes simplex virus infection. *Trends Microbiol.* 12:353–356.
21. Edelmann, K.H., S. Richardson-Burns, L. Alexopoulou, K.L. Tyler, R.A. Flavell, and M.B. Oldstone. 2004. Does Toll-like receptor 3 play a biological role in virus infections? *Virology*. 322:231–238.
22. Lund, J.M., L. Alexopoulou, A. Sato, M. Karow, N.C. Adams, N.W. Gale, A. Iwasaki, and R.A. Flavell. 2004. Recognition of single-stranded RNA viruses by Toll-like receptor 7. *Proc. Natl. Acad. Sci. USA*. 101:5598–5603.
23. Lund, J., A. Sato, S. Akira, R. Medzhitov, and A. Iwasaki. 2003. Toll-like receptor 9-mediated recognition of Herpes simplex virus-2 by plasmacytoid dendritic cells. *J. Exp. Med.* 198:513–520.
24. Pfeffer, L.M., C.A. Dinarello, R.B. Herberman, B.R. Williams, E.C. Borden, R. Bordens, M.R. Walter, T.L. Nagabhushan, P.P. Trotta, and S. Pestka. 1998. Biological properties of recombinant alpha-interferons: 40th anniversary of the discovery of interferons. *Cancer Res.* 58:2489–2499.
25. van den Broek, M., U. Muller, S. Huang, R. Zinkernagel, and M. Auget. 1995. Immune defence in mice lacking type I and/or type II interferon receptors. *Immunol. Rev.* 148:5–18.
26. Biron, C.A. 2001. Interferons alpha and beta as immune regulators–a new look. *Immunity*. 14:661–664.
27. Honda, K., S. Sakaguchi, C. Nakajima, A. Watanabe, H. Yanai, M. Matsumoto, T. Ohteki, T. Kaisho, A. Takaoka, S. Akira, et al. 2003. Selective contribution of IFN-alpha/beta signaling to the maturation of dendritic cells induced by double-stranded RNA or viral infection. *Proc. Natl. Acad. Sci. USA*. 100:10872–10877. Epub 12003 Sep 10875.
28. Hoshino, K., T. Kaisho, T. Iwabe, O. Takeuchi, and S. Akira. 2002. Differential involvement of IFN-beta in Toll-like receptor-stimulated dendritic cell activation. *Int. Immunol.* 14:1225–1231.
29. De Trez, C., M. Brait, O. Leo, T. Aebischer, F.A. Torrentera, Y. Carlier, and E. Muraille. 2004. Myd88-dependent in vivo maturation of splenic dendritic cells induced by *Leishmania donovani* and other Leishmania species. *Infect. Immun.* 72:824–832.
30. Reis e Sousa, C., S. Hieny, T. Scharton-Kersten, D. Jankovic, H. Charest, R.N. Germain, and A. Sher. 1997. In vivo microbial stimulation induces rapid CD40 ligand-independent production of interleukin 12 by dendritic cells and their redistribution to T cell areas. *J. Exp. Med.* 186:1819–1829.
31. Asselin-Paturel, C., G. Brizard, J.J. Pin, F. Briere, and G. Trinchieri. 2003. Mouse strain differences in plasmacytoid dendritic cell frequency and function revealed by a novel monoclonal antibody. *J. Immunol.* 171:6466–6477.

32. Krug, A., R. Uppaluri, F. Facchetti, B.G. Dorner, K.C. Sheehan, R.D. Schreiber, M. Cella, and M. Colonna. 2002. IFN-producing cells respond to CXCR3 ligands in the presence of CXCL12 and secrete inflammatory chemokines upon activation. *J. Immunol.* 169:6079–6083.
33. Penna, G., M. Vulcano, S. Sozzani, and L. Adorini. 2002. Differential migration behavior and chemokine production by myeloid and plasmacytoid dendritic cells. *Hum. Immunol.* 63:1164–1171.
34. Jarrossay, D., G. Napolitani, M. Colonna, F. Sallusto, and A. Lanzavecchia. 2001. Specialization and complementarity in microbial molecule recognition by human myeloid and plasmacytoid dendritic cells. *Eur. J. Immunol.* 31:3388–3393.
35. Montoya, M., G. Schiavoni, F. Mattei, I. Gresser, F. Belardelli, P. Borrow, and D.F. Tough. 2002. Type I interferons produced by dendritic cells promote their phenotypic and functional activation. *Blood.* 99:3263–3271.
36. Luft, T., K.C. Pang, E. Thomas, P. Hertzog, D.N. Hart, J. Trapani, and J. Cebon. 1998. Type I IFNs enhance the terminal differentiation of dendritic cells. *J. Immunol.* 161:1947–1953.
37. Steinman, R.M., M. Pack, and K. Inaba. 1997. Dendritic cells in the T-cell areas of lymphoid organs. *Immunol. Rev.* 156:25–37.
38. Eloranta, M.L., and G.V. Alm. 1999. Splenic marginal metallophilic macrophages and marginal zone macrophages are the major interferon-alpha/beta producers in mice upon intravenous challenge with herpes simplex virus. *Scand. J. Immunol.* 49:391–394.
39. Penna, G., S. Sozzani, and L. Adorini. 2001. Cutting edge: selective usage of chemokine receptors by plasmacytoid dendritic cells. *J. Immunol.* 167:1862–1866.
40. Vanbervliet, B., N. Bendriss-Vermare, C. Massacrier, B. Homey, O. de Bouteiller, F. Briere, G. Trinchieri, and C. Caux. 2003. The inducible CXCR3 ligands control plasmacytoid dendritic cell responsiveness to the constitutive chemokine stromal cell-derived factor 1 (SDF-1)/CXCL12. *J. Exp. Med.* 198:823–830.
41. Yoneyama, H., K. Matsuno, Y. Zhang, T. Nishiwaki, M. Kitabatake, S. Ueha, S. Narumi, S. Morikawa, T. Ezaki, B. Lu, et al. 2004. Evidence for recruitment of plasmacytoid dendritic cell precursors to inflamed lymph nodes through high endothelial venules. *Int. Immunol.* 16:915–928.
42. Megjugorac, N.J., H.A. Young, S.B. Amrute, S.L. Olshalsky, and P. Fitzgerald-Bocarsly. 2004. Virally stimulated plasmacytoid dendritic cells produce chemokines and induce migration of T and NK cells. *J. Leukoc. Biol.* 75:504–514.
43. Padovan, E., G.C. Spagnoli, M. Ferrantini, and M. Heberer. 2002. IFN-alpha2a induces IP-10/CXCL10 and MIG/CXCL9 production in monocyte-derived dendritic cells and enhances their capacity to attract and stimulate CD8+ effector T cells. *J. Leukoc. Biol.* 71:669–676.